Journal of Sound and Vibration (2002) **255**(1), 43–59
doi:10.1006/jsvi.2001.4151, available online at http://www.idealibrary.com on IDEAL®

NON-LINEAR DYNAMIC ANALYSIS OF THE TWO-DIMENSIONAL SIMPLIFIED MODEL OF AN ELASTIC CABLE

Y. Y. Zhao, L. H. Wang and D. L. Chen

The Department of Engineering Mechanics, Hunan University, Changsha, Hunan, 410082, People's Republic of China. E-mail: yyzhao@mail.hunu.edu.cn

AND

L. Z. Jiang

School of Civil and Architecture Engineering, Central South University, Changsha, Hunan, 410075, *People's Republic of China*

(*Received* 10 *January* 2001, *and in final form* 5 *September* 2001)

The non-linear behavior of an elastic cable subjected to a harmonic excitation is investigated in this paper. Using Garlerkin's method and method of multiple scales, the discrete dynamical equations and a set of first order non-linear differential equations are obtained. A numerical simulation is used to obtain the steady state response and stable solutions. Finally the coupled dynamic features between the out-planar pendulation and the in-planar vibration of an elastic cable are analyzed.

1. INTRODUCTION

The cable is featured by its flexibility, lightness and light damping. For this superior structure, cables are very efficient structural members and hence have been widely used in many long-span structures, including cable-supported bridges, guyed towers and cable-supported roofs. So the dynamic study of the cable is of great engineering significance. Generally speaking, the non-linear feature results from material, large deformation and sag. And the dynamic study of the cable is very complicated and remains a key research field of mathematics, mechanics, and engineering. Yamaguchi, *et al.* [1] studied the time response of a cable under harmonic excitation and they concluded that the dynamic of cable was greatly influenced by geometric and physics parameters. A numerical hybrid method was used by Yu and Xu [2] to formulate three-dimensional small-amplitude free and forced vibration problems of an inclined sag cable equipped with discrete oil dampers. Effects of non-linearity on planar/non-planar dynamic motion of a sagged cable were investigated by Hagedam and Shafer [3]. Rao and Iyengar [4] made a study of the internal resonance and non-linear response under periodic excitation. The dynamic stability problem of a flag sag cable subjected to an axial periodic load was investigated by Takahashi [5]. Perkins [6] studied the non-linear response of the model interactions under parametric and forced excitation. To simplify the procedure of designing viscous dampers for stay cables in bridges, Benito *et al.* [7] proposed a universal estimation curve that related the modal damping ratio of the cable. Benedethni, *et al.* [8] conducted research in the non-linear

0022-460X/02/$35.00

oscillation of a four-degree-of-freedom (d.o.f.) model of a suspended cable under multiple internal resonance conditions. Taking geometric non-linearity into consideration, Zhao [9] established three-dimensional dynamical equations of cables by applying the Newton's method, and studied the dynamic features of cables.

In this study, a three-dimensional problem based on reference [9, 10] is reduced to a two-dimensional one. And internal resonance of 1:1 is considered. Applying Galerkin's method, the two-dimensional discrete dynamical equations are obtained, and the method of multiple scales is used to reduce the differential equations to a set of first order differential equations that are solved by Newton's method, and the fixed-point response curves are also investigated. In the end, the coupled dynamic features between the out-planar pendulation and the in-planar vibration of an elastic cable are analyzed.

2. ANALYSIS OF THE TWO-DIMENSIONAL CABLE

2.1. THE SIMPLIFIED EQUATION

This study deals with the coupling of the out-planar pendulation and the in-planar vibration of an inclined sag cable. The uniform cable is assumed to have small amplitude vibration with respect to its static equilibrium position and have very small sag (Figure 1). By setting the x- and y- co-ordinate in the static profile plane of the cable and taking the left support of the cable as the origin of the Cartesian co-ordinate system, the partial differential equations of the cable motion can be written as [9, 10] (not including the effect of viscous damping)

$$\frac{\partial}{\partial x}\left\{\left[(N_0 - EA)\frac{\mathrm{d}x}{\mathrm{d}s} + \frac{1}{\sqrt{1 + y_x^2}}EA\right](1 + u_x)\right\} = \rho A u_{tt}, \tag{1a}$$

$$\frac{\partial}{\partial x}\left\{\left[(N_0 - EA)\frac{\mathrm{d}x}{\mathrm{d}s} + \frac{1}{\sqrt{1 + y_x^2}}EA\right](w_x + y_x)\right\} = \rho A w_{tt}, \tag{1b}$$

$$\frac{\partial}{\partial x}\left\{\left[(N_0 - EA)\frac{\mathrm{d}x}{\mathrm{d}s} + \frac{1}{\sqrt{1 + y_x^2}}EA\right]v_x\right\} = \rho A v_{tt}, \tag{1c}$$

where N_0 is the static cable tension, u, w and v are axial, in-plane transverse and out-plane transverse displacements of the cable respectively, E is Young's modulus, A is the area of the cross-section, ρ is the density of the cable, y is the static equilibrium of the cable, s is the Lagrangian co-ordinate in the unstrained cable profile, $(\ )_x$ denotes partial differentiation with respect to x, $(\ )_t$ denotes partial differentiation with respect to time t, $\mathrm{d}x/\mathrm{d}s$ can be written as

$$\frac{\mathrm{d}x}{\mathrm{d}s} = \frac{1}{\sqrt{(1 + u_x)^2 + (w_x + y_x)^2 + v_x^2}}. \tag{2}$$

For the development of an approximate theory for the cable, the following assumptions are adopted: $O(u) \ll O(w)$; $O(u_x) \ll O(w_x)$; $O(u_x) \ll O(v_x)$; $O(u_x) \ll O(y_x)$; u_x, w_x, y_x are all small with respect to 1. Using the Taylor series expansion and retaining only the lower order non-linear terms, we can obtain

$$\frac{\mathrm{d}x}{\mathrm{d}s} \approx 1 - e - \tfrac{1}{2}y_x^2, \quad e = u_x + y_x w_x - u_x^2 + \tfrac{1}{2}v_x^2 + \tfrac{1}{2}w_x^2. \tag{3}$$

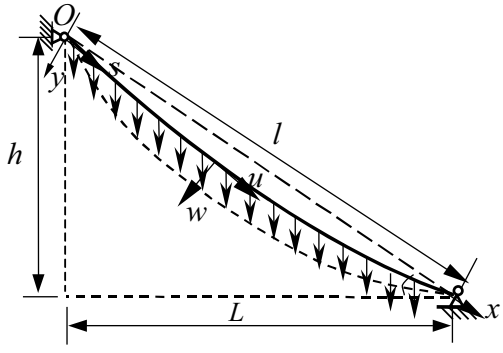

Figure 1. The three-dimensional model of the cable.

Substituting equations (3) into equations (1) and using the Taylor series expansion, we can obtain

$$u_{tt} + \frac{1}{\rho A}\frac{\partial}{\partial x}[(N_0 - EA)e] - \frac{1}{\rho A}\frac{\partial}{\partial x}\left[N_0\left(1 - \frac{y_x^2}{2}\right)u_x\right] + \frac{1}{\rho A}\frac{\partial}{\partial x}[(N_0 - EA)u_x e] = 0, \tag{4a}$$

$$w_{tt} + \frac{1}{\rho A}\frac{\partial}{\partial x}[(N_0 - EA)ew_x] - \frac{1}{\rho A}\frac{\partial}{\partial x}\left[N_0\left(1 - \frac{y_x^2}{2}\right)w_x\right] + \frac{1}{\rho A}\frac{\partial}{\partial x}[(N_0 - EA)ey_x] = 0, \tag{4b}$$

$$v_{tt} - \frac{1}{\rho A}\frac{\partial}{\partial x}\left[N_0\left(1 - \frac{y_x^2}{2}\right)u_x\right] + \frac{1}{\rho A}\frac{\partial}{\partial x}[(N_0 - EA)v_x e] = 0, \tag{4c}$$

where the terms irrelative to time t have been ignored for the convenience of the study. Introducing the non-dimensional time t^* defined as

$$t^* = \sqrt{\frac{H_0}{\rho A l}}\, t, \tag{5}$$

where l represents the span of the cable and H_0 is the horizontal tension, we can obtain

$$u_{tt} + \frac{l}{H_0}\frac{\partial}{\partial x}[(N_0 - EA)e] - \frac{l}{H_0}\frac{\partial}{\partial x}\left[N_0\left(1 - \frac{y_x^2}{2}\right)u_x\right] + \frac{l}{H_0}\frac{\partial}{\partial x}[(N_0 - EA)u_x e] = 0, \tag{6a}$$

$$w_{tt} + \frac{l}{H_0}\frac{\partial}{\partial x}[(N_0 - EA)ew_x] - \frac{l}{H_0}\frac{\partial}{\partial x}\left[N_0\left(1 - \frac{y_x^2}{2}\right)w_x\right] + \frac{l}{H_0}\frac{\partial}{\partial x}[(N_0 - EA)ey_x] = 0, \tag{6b}$$

$$v_{tt} - \frac{l}{H_0}\frac{\partial}{\partial x}\left[N_0\left(1 - \frac{y_x^2}{2}\right)u_x\right] + \frac{l}{H_0}\frac{\partial}{\partial x}[(N_0 - EA)v_x e] = 0, \tag{6c}$$

where the * notation has been disposed. In the following, the in-planar motion is reduced for the sake of studying the coupling between out-planar pendulation and in-planar

vibration. If we only consider the lower order transverse modes, no interaction will occur between these transverse modes and the longitudinal modes, and the longitudinal inertia u_{tt} can be neglected [11]. As a consequence from equation (6a), we can obtain

$$-(N_0 - EA)e + N_0\left(1 - \frac{y_x^2}{2}\right)u_x - (N_0 - EA)u_x e \approx P(t), \tag{7}$$

where $P(t)$ is a variable only relative to time t. Taking into consideration $u_x = O(w_x^2)$ and $N_0/EA = \sigma/E \ll 1$, we can obtain

$$(u_x + y_x w_x + \tfrac{1}{2}v_x^2 + \tfrac{1}{2}w_x^2) \approx G(t), \tag{8}$$

where $G(t) = P(t)/EA$, with boundary conditions of cable $u(0) = u(l) = 0$ applied, we can obtain

$$G(t) \approx \frac{1}{l}\int_0^l (y_x w_x + \tfrac{1}{2}v_x^2 + \tfrac{1}{2}w_x^2)\,dx. \tag{9}$$

Substituting equation (9) into equation (8), we can obtain

$$u_x \approx G(t) - (y_x w_x + \tfrac{1}{2}v_x^2 + \tfrac{1}{2}w_x^2). \tag{10}$$

Substituting $e = G(t) = e(t)$ derived from equations (3) and equations (8) into equations (1), the two-dimensional equations reduced from three-dimensional ones can be realized as

$$w_{tt} - \frac{l}{H_0}\frac{\partial}{\partial x}\left\{N_0\left(1 - \frac{y_x^2}{2}\right)w_x - (N_0 - EA)\mathrm{e}(t)w_x - (N_0 - EA)\mathrm{e}(t)y_x\right\} = 0, \tag{11a}$$

$$v_{tt} - \frac{l}{H_0}\frac{\partial}{\partial x}\left\{N_0\left(1 - \frac{y_x^2}{2}\right)v_x - (N_0 - EA)\mathrm{e}(t)v_x\right\} = 0. \tag{11b}$$

For the purpose of the analysis of equations (11), the Galerkin's procedure is introduced. Based on hypothesis $w(x, t) = q_2(t)\varphi_2(x)$ and $v(x, t) = q_3(t)\varphi_3(x)$, and introducing viscous damping and external excitation, we can obtain

$$\begin{aligned}&\int_0^l \ddot{q}_2\varphi_2^2(x)\,\mathrm{d}x + 2\int_0^l c_2\dot{q}_2\varphi_2^2(x)\,\mathrm{d}x - \frac{1}{H_0}\int_0^l \frac{\partial}{\partial x}\left[N_0\left(1 - \frac{y_x^2}{2}\right)q_2\varphi_{2x}\right]\varphi_2(x)\,\mathrm{d}x\\ &+ \frac{l}{H_0}\int_0^l \frac{\partial}{\partial x}[(N_0 - EA)e(t)q_2\varphi_{2x}]\varphi_2(x)\,\mathrm{d}x + \frac{1}{H_0}\int_0^l \frac{\partial}{\partial x}[(N_0 - EA)e(t)y_x]\varphi_2(x)\,\mathrm{d}x = 0,\end{aligned} \tag{12a}$$

$$\begin{aligned}&\int_0^l \ddot{q}_3\varphi_3^2(x)\,\mathrm{d}x + 2\int_0^l c_3\dot{q}_3\varphi_3^2(x)\,\mathrm{d}x - \frac{l}{H_0}\int_0^l \frac{\partial}{\partial x}\left[N_0\left(1 - \frac{y_x^2}{2}\right)q_3\varphi_{3x}\right]\varphi_3(x)\,\mathrm{d}x\\ &+ \frac{l}{H_0}\int_0^l \frac{\partial}{\partial x}[(N_0 - EA)e(t)q_3\varphi_{3x}]\varphi_3(x)\,\mathrm{d}x = \int_0^l F(x, t)\varphi_3(x)\,\mathrm{d}x,\end{aligned} \tag{12b}$$

where the overdot indicates differentiation with respect to time t, c_2, c_3 are the damping coefficients;

$$e(t) = \frac{q_2}{l}\int_0^l y_x\varphi_{2x}\,\mathrm{d}x + \frac{q_2^2}{2l}\int_0^l \varphi_{2x}^2\,\mathrm{d}x + \frac{q_3^2}{2l}\int_0^l \varphi_{3x}^2\,\mathrm{d}x. \tag{13}$$

Substituting equation (13) into equations (12) and keeping up to cubic terms, we can obtain

$$b_1\ddot{q}_2 + b_2q_2 + b_3q_2^2 + b_4q_3^2 + b_5q_2^3 + b_6q_3^2q_2 + \zeta_2\dot{q}_2 = 0, \tag{14a}$$

$$c_1\ddot{q}_3 + c_2q_3 + c_3q_2q_3 + c_4q_2^2q_3 + c_5q_3^3 + \zeta_3\dot{q}_3 = Q(t), \tag{14b}$$

where the coefficients are written in Appendix A.

For the convenience of the analysis of equations (14), the non-dimensional parameter ε is introduced, and the external excitation is noted as $Q(t) = Q_0 \cos \Omega t$, where Q_0 and Ω are amplitude and the frequency of the excitation, respectively. We can obtain

$$\ddot{q}_2 + 2\varepsilon\mu_2\dot{q}_2 + \omega_2^2q_2 + \varepsilon\alpha_2q_2^2 + \varepsilon\beta_2q_3^2 + \varepsilon\gamma_2q_2^3 + \varepsilon\eta_2q_3^2q_2 = 0, \tag{15a}$$

$$\ddot{q}_3 + 2\varepsilon\mu_3\dot{q}_3 + \omega_3^2q_3 + \varepsilon\alpha_3q_2q_3 + \varepsilon\gamma_3q_3^3 + \varepsilon\eta_3q_2^2q_3 = 2\varepsilon f_3 \cos \Omega t, \tag{15b}$$

where $\omega_2^2 = b_2/b_1$, $\varepsilon\alpha_2 = b_3/b_1$, $\varepsilon\beta_2 = b_4/b_1$, $\varepsilon\gamma_2 = b_5/b_1$, $\varepsilon\eta_2 = b_6/b_1$, $2\varepsilon\mu_2 = \zeta_2/b_1$, $\omega_3^2 = c_2/c_1$, $\varepsilon\alpha_3 = c_3/c_1$, $\varepsilon\gamma_3 = c_4/c_1$, $\varepsilon\eta_3 = c_5/c_1$, $2\varepsilon\mu_3 = \zeta_3/c_1$, $2\varepsilon f_3 \cos \Omega t = Q_0/c_1$.

2.2. PERTURBATION SOLUTION

The approximate solution of equations (15) can be obtained by using the method of multiple scales [12]. Let

$$q_i(t; \varepsilon) = q_{i0}(T_0, T_1) + \varepsilon q_{i1}(T_0, T_1) + O(\varepsilon^2), \quad i = 1, 2, \tag{16}$$

where $T_i = \varepsilon^i t$, therefore,

$$\frac{\mathrm{d}}{\mathrm{d}t} = \frac{\partial}{\partial T_0} + \varepsilon\frac{\partial}{\partial T_1} + \cdots = D_0 + \varepsilon D_1 + \cdots, \tag{17a}$$

$$\frac{\mathrm{d}^2}{\mathrm{d}t^2} = \frac{\partial^2}{\partial T_0^2} + 2\varepsilon\frac{\partial^2}{\partial T_0 \partial T_1} + \cdots = D_0^2 + 2\varepsilon D_0D_1 + \cdots, \tag{17b}$$

where $D_0 = \partial/\partial T_0$, $D_1 = \partial/\partial T_1$. Substituting equations (16) and equations (17) into equations (15) and equating the coefficients of ε^0 and ε^1 to zero, we can obtain

$$\varepsilon^0: \quad D_0^2q_{20} + \omega_2^2q_{20} = 0, \qquad D_0^2q_{30} + \omega_3^2q_{30} = 0, \tag{18a,b}$$

$$\varepsilon^1: \quad D_0^2q_{21} + \omega_2^2q_{21} + 2D_0D_1q_{20} + 2\mu_2D_0q_{20} + \alpha_2q_{20}^2 + \beta_2q_{30}^2 + \gamma_2q_{20}^3 + \eta_2q_{20}q_{30}^2 = 0, \tag{19a}$$

$$D_0^2q_{31} + \omega_3^2q_{31} + 2D_0D_1q_{30} + 2\mu_3D_0q_{30} + \alpha_3q_{20}q_{30} + \gamma_3q_{30}^3 + \eta_3q_{20}^2q_{30} = 2f_3 \cos \Omega t. \tag{19b}$$

The solutions for equations (18) can be expressed as

$$q_{20} = A_2(T_1)\mathrm{e}^{\mathrm{i}\omega_2T_0} + \bar{A}_2\mathrm{e}^{-\mathrm{i}\omega_2T_0}, \tag{20a}$$

$$q_{30} = A_3(T_1)\mathrm{e}^{\mathrm{i}\omega_3T_0} + \bar{A}_3\mathrm{e}^{-\mathrm{i}\omega_3T_0}, \tag{20b}$$

where A_n are unknown functions of T_1, $\bar{A}_n$ are the complex conjugates of A_n.

Substituting equations (20) into equations (19), we can obtain

$$D_0^2q_{21} + \omega_2^2q_{21} = -2\mathrm{i}\omega_2(A_2' + \mu_2A_2)\mathrm{e}^{\mathrm{i}\omega_2T_0} - \alpha_2A_2\bar{A}_2 - \alpha_2A_2^2\mathrm{e}^{2\mathrm{i}\omega_2T_0} - \beta_2A_3^2\mathrm{e}^{2\mathrm{i}\omega_3T_0} - \gamma_2A_2^3\mathrm{e}^{3\mathrm{i}\omega_0T_0} - \eta_2\bar{A}_3^2A_2\mathrm{e}^{\mathrm{i}(\omega_2-2\omega_3)T_0}$$

$$- \beta_2 A_3 \bar{A}_3 - 2\eta_2 A_3 \bar{A}_3 A_2 e^{i\omega_2 T_0} - \eta_2 A_3^2 A_2 e^{i(2\omega_3+\omega_2)T_0}$$
$$- 3\gamma_2 A_2^2 \bar{A}_2 e^{i\omega_2 T_0} + cc, \tag{21a}$$

$$D_0^2 q_{31} + \omega_3^2 q_{31} = - 2i\omega_3(A_3' + \mu_3 A_3)e^{i\omega_3 T_0} - \alpha_3 A_2 A_3 e^{i(\omega_2+\omega_3)T_0}$$
$$- \alpha_3 A_2 \bar{A}_3 e^{i(\omega_2-\omega_3)T_0} - \gamma_3 A_3^3 e^{3i\omega_3 T_0} - 3\gamma_3 \bar{A}_3 A_3^2 e^{i\omega_3 T_0}$$
$$- \eta_3 A_3 A_2^2 e^{i(\omega_3+2\omega_2)T_0} - 2\eta_3 A_3 A_2 \bar{A}_2 e^{i\omega_3 T_0}$$
$$- \eta_3 \bar{A}_2^2 A_3 e^{i(\omega_3-2\omega_2)T_0} + f_3 e^{i\Omega T_0} + cc, \tag{21b}$$

where cc indicates the complex conjugate of the preceding terms, and the function A_n can be determined by the requirement that solutions to equations (21) do not contain secular terms, or small-divisor terms caused by resonance. And the internal resonance conditions are $\omega_2 \approx \omega_3$ and $\omega_2 \approx 2\omega_3$. For the case $\Omega = \omega_3 + \varepsilon\sigma$ with ω_2 away from ω_3 and $2\omega_3$, the solvability conditions of equations (21) are derived as

$$- 2i\omega_2(A_2' + \mu_2 A_2) - 2\eta_2 A_2 A_3 \bar{A}_3 - 3\gamma_2 A_2^2 \bar{A}_2 = 0, \tag{22a}$$

$$- 2i\omega_3(A_3' + \mu_3 A_3) - 3\gamma_3 A_3^2 \bar{A}_3 - 2\eta_3 A_3 A_2 \bar{A}_2 + f_3 e^{i\sigma T_1} = 0. \tag{22b}$$

Letting $A_2 = \frac{1}{2} a_2 e^{i\theta_2}$, $A_3 = \frac{1}{2} a_3 e^{i\theta_3}$ in equations (22), and separating into real and imaginary parts, we can obtain

$$a_2' = - \mu_2 a_2, \tag{23a}$$

$$a_2\theta_2' = \frac{\eta_2}{4\omega_2} a_2 a_3^2 + \frac{3\gamma_2}{8\omega_2} a_2^3, \tag{23b}$$

$$a_3' = - \mu_3 a_3 + \frac{f_3}{\omega_3} \sin\lambda, \tag{23c}$$

$$a_3\theta_3' = \frac{3\gamma_3 a_3^3}{8\omega_3} + \frac{\eta_3}{4\omega_3} a_3 a_2^2 - \frac{f_3}{\omega_3} \cos\lambda, \tag{23d}$$

where $\lambda = \sigma T_1 - \theta_3$. And a prime denotes the derivative with respect to T_1. Since the motion in planar is neither directly excited by external excitation nor indirectly excited by internal resonance, it can be shown that the response amplitude of the motion in-planar dies out due to the presence of damping.

In the following, the case $\Omega \approx \omega_3$ with $\omega_2 \approx \omega_3$ is discussed. To express the proximity of ω_2 to ω_3, the detuning parameter σ_1 is introduced. Also, to account for the internal resonance, the detuning σ_2 is used. We have

$$\omega_2 = \omega_3 + \varepsilon\sigma_1, \ \Omega = \omega_3 + \varepsilon\sigma_2.$$

Eliminating the terms that produce a secular term in equations (21), the solvability conditions are derived as

$$- 2i\omega_2(A_2' + \mu_2 A_2) - \eta_2 A_3^2 \bar{A}_2 e^{-2i\sigma_1 T_1} - 2\eta_2 A_3 \bar{A}_3 A_2 - 3\gamma_2 A_2^2 \bar{A}_2 = 0, \tag{24a}$$

$$- 2i\omega_3(A_3' + \mu_3 A_3) - 2\eta_3 A_3 A_2 \bar{A}_2 - \eta_3 A_2^2 \bar{A}_3 e^{2i\sigma_1 T_1} - 3\gamma_3 A_3^2 \bar{A}_3 + f_3 e^{i\sigma_2 T_1} = 0, \tag{24b}$$

where a prime denotes the derivative with respect to T_1.

To solve equations (24), A_n are expressed in the polar forms

$$A_2 = \tfrac{1}{2} a_2 e^{i\theta_2}, \qquad A_3 = \tfrac{1}{2} a_3 e^{i\theta_3}, \tag{25}$$

where a_2, a_3, θ_2, θ_3 are real. Substituting equations (25) into equations (24) and separating real and imaginary parts, one can obtain the following equations:

$$a_2' = -\mu_2 a_2 - \frac{\eta_2 a_3^2 a_2}{8\omega_2}\sin(2\lambda_2 - 2\lambda_3), \tag{26a}$$

$$a_3' = -\mu_3 a_3 + \frac{\eta_3 a_2^2 a_3}{8\omega_3}\sin(2\lambda_2 - 2\lambda_3) + \frac{f_3}{\omega_3}\sin\lambda_3, \tag{26b}$$

$$a_2(\sigma_2 - \sigma_1 - \lambda_2') = \frac{\eta_2 a_3^2 a_2}{4\omega_2} + \frac{3\gamma_2 a_2^3}{8\omega_2} + \frac{\eta_2 a_3^2 a_2}{8\omega_2}\cos(2\lambda_2 - 2\lambda_3), \tag{26c}$$

$$a_3(\sigma_2 - \lambda_3') = \frac{3\gamma_3 a_3^3}{8\omega_3} + \frac{\eta_3 a_3 a_2^2}{4\omega_3} + \frac{\eta_3 a_2^2 a_3}{8\omega_3}\cos(2\lambda_2 - 2\lambda_3) - \frac{f_3}{\omega_3}\cos\lambda_3, \tag{26d}$$

where $\lambda_2 = (\sigma_2 - \sigma_1)T_1 - \theta_2, \lambda_3 = \sigma_2 T_1 - \theta_3$.

The above equations are known as the reduced equations. For steady state, $a_2' = a_3' = \lambda_2' = \lambda_3' = 0$. So now, we have a set of non-linear algebraic equations that are solved numerically to obtain the fixed-point response of the system. In this case, two types of solutions are possible, namely: (1) $a_2 = 0, a_3 \neq 0$, the motion is out of the plane and under these circumstances, the cable is subject to pendulation; (2) $a_2 \neq 0$, $a_3 \neq 0$, the motion is of non-planar, out-planar pendulation and in-plane vibration coupling.

For steady state out-planar motion, equations (26) can be combined into

$$\frac{f_3^2}{\omega_3^2} = \mu_3^2 a_3^2 + \left(a_3\sigma_2 - \frac{3\gamma_3}{8\omega_3}a_3^3\right)^2. \tag{27}$$

Thus, this system is equivalent to a hardening spring-mass system. However, when the response amplitude exceeds a critical value, the out-planar motion becomes unstable, and the motion becomes non-planar.

In the second case, equations (23) can be combined into

$$\mu_2 a_2 + \frac{\eta_2 a_3^2 a_2}{8\omega_2}\sin(2\lambda_2 - 2\lambda_3) = 0, \tag{28a}$$

$$-\mu_3 a_3 + \frac{\eta_3 a_2^2 a_3}{8\omega_3}\sin(2\lambda_2 - 2\lambda_3) + \frac{f_3}{\omega_1}\sin\lambda_3 = 0, \tag{28b}$$

$$\frac{\eta_2 a_3^2 a_2}{4\omega_3} + \frac{3\gamma_2 a_2^3}{8\omega_2} + \frac{\eta_2 a_3^2 a_2}{8\omega_2}\cos(2\lambda_2 - 2\lambda_3) = a_2(\sigma_2 - \sigma_1), \tag{28c}$$

$$\frac{3\gamma_3 a_3^3}{8\omega_3} + \frac{\eta_3 a_3 a_2^2}{4\omega_3} + \frac{\eta_3 a_3 a_2^2}{8\omega_3}\cos(2\lambda_2 - 2\lambda_3) - \frac{f_3}{\omega_3}\cos\lambda_3 = a_3\sigma_2. \tag{28d}$$

In this case, these equations can be solved for a_2, a_3, λ_2 and λ_3 using a Newton-Raphson method. Thus, the first order solution of the system can be given by

$$q_2 = a_2\cos\{[\omega_2 + \varepsilon(\sigma_2 - \sigma_1)]t - \lambda_2\}, \tag{29a}$$

$$q_3 = a_3\cos[(\omega_2 + \varepsilon\sigma_2)t - \lambda_3]. \tag{29b}$$

From equations (29), we know that the non-linearity adjusts the frequencies so that they are precise equalities. This can be shown as follows:

$$\omega_2 T_0 + \theta_2 = \omega_2 T_0 + \varepsilon(\sigma_2 - \sigma_1)t - \lambda_2 = \Omega t - \lambda_2, \tag{30a}$$

$$\omega_3 T_0 + \theta_3 = \omega_3 T_0 + \varepsilon\sigma_2 t - \lambda_3 = \Omega t - \lambda_3. \tag{30b}$$

Thus, the deflections of the cable are given by

$$w(x, t) = a_2 \cos(\Omega t - \lambda_2)\varphi_2(x) + O(\varepsilon), \tag{31a}$$

$$v(x, t) = a_3 \cos(\Omega t - \lambda_3)\varphi_3(x) + O(\varepsilon). \tag{31b}$$

2.3. STABILITY EQUATIONS OF STEADY STATE RESPONSE

By directly perturbing the reduced equations, one can study the stability of the non-trivial steady state solutions. But, as the reduced equations have the coupled terms $a_2\lambda_2'$ and $a_3\lambda_3'$, the perturbed equations will not contain perturbation $\Delta\lambda_2'$ for trivial solutions and hence the stability of the trivial state cannot be studied by directly perturbing equations (26). Hence, to overcome this difficulty, introducing the transformations

$$p_i = a_i \cos\lambda_i, \quad q_i = a_i \sin\lambda_i, \qquad i = 2, 3 \tag{32}$$

and carrying out trigonometric manipulations, one arrives at the following normalized reduced equations:

$$\omega_2[p_2' + (\sigma_2 - \sigma_1)q_2 + \mu_2 p_2] + \frac{\eta_2}{8}[(p_3^2 - q_3^2)q_2 - 2p_3q_3p_2] - \frac{\eta_2}{4}(p_3^2 + q_3^2)q_2 - \frac{3\gamma_2}{8}q_2(p_2^2 + q_2^2) = 0, \tag{33a}$$

$$\omega_2[q_2' - (\sigma_2 - \sigma_1)p_2 + \mu_2 q_2] + \frac{\eta_2}{8}[(p_3^2 - q_3^2)p_2 + 2p_3q_3q_2] + \frac{\eta_2}{4}(p_3^2 + q_3^2)p_2 - \frac{3\gamma_2}{8}p_2(p_2^2 + q_2^2) = 0, \tag{33b}$$

$$\omega_3[p_3' + \sigma_2 q_3 + \mu_3 p_3] - \frac{\eta_3}{8}[(p_2^2 - q_2^2)q_3 - 2p_2q_2p_3] - \frac{\eta_3}{4}(p_2^2 + q_2^2)q_3 - \frac{3\gamma_3}{8}q_3(p_3^2 + q_3^2) = 0, \tag{33c}$$

$$\omega_3[q_3' - \sigma_2 p_3 + \mu_3 q_3] + \frac{\eta_3}{8}[(p_2^2 - q_2^2)p_3 + 2p_2q_2q_3] + \frac{\eta_3}{4}(p_2^2 + q_2^2)p_3 + \frac{3\gamma_3}{8}p_3(p_3^2 + q_3^2) - f_3 = 0. \tag{33d}$$

To determine which of the various possible solutions are stable, we perturb the steady state solution. That is

$$p_2 = p_{20} + \Delta p_2, \quad p_3 = p_{30} + \Delta p_3, \quad q_2 = q_{20} + \Delta q_2, \quad q_3 = q_{30} + \Delta q_3,$$

where the subscript 0 indicates the steady values and Δ indicates the perturbation values. Substituting them into equations (32) and retaining linear terms in the perturbation, we obtain

$$\{\Delta p_2', \Delta q_2', \Delta p_3', \Delta q_3'\}^{\mathrm{T}} = [J_c]\{\Delta p_2, \Delta q_2, \Delta p_3, \Delta q_3\}^{\mathrm{T}}, \tag{34}$$

where T is the transpose and $[J_c]$ is the Jacobian matrix whose eigenvalues will determine the stability and bifurcation of the system.

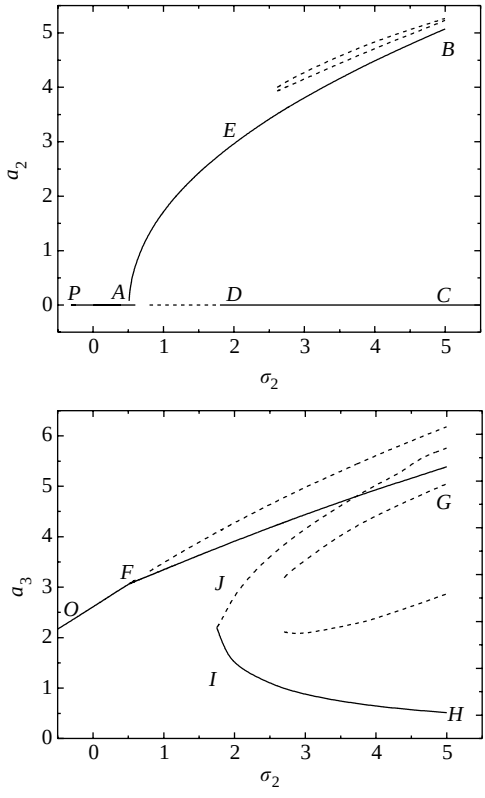

Figure 2. Frequency–response curve for a cable for the case of a primary resonance of the first mode: $f_3 = 0{\cdot}85$, $\mu_2 = 0{\cdot}2$, $\mu_3 = 0{\cdot}2$.

3. NUMERICAL RESULTS AND DISCUSSION

An elastic cable which is simply supported is treated in the following numerical examples with the following properties: $f = 0{\cdot}25$m, $H_0 = 3{\cdot}5 \times 10^6$ N, $\rho A = 20{\cdot}96$ kg/m, $A = 2{\cdot}635 \times 10^{-3}$ m^2, $h = 50$ m, $L = 100$ m, $E = 1{\cdot}95 \times 10^{11}$N/m^2, where the definition of sag f, expression of the static equilibrium of the cable and static cable tension have been given by reference [13]. To the simply supported cable, the mode shapes can be given by $\varphi_2(x) = \sin(\pi x/l)$, $\varphi_3(x) = \sin(\pi x/l)$. The corresponding natural frequencies are $\omega_2 = 0{\cdot}314408$ and $\omega_3 = 0{\cdot}314159$. The parameter ε is taken as $\varepsilon = 0{\cdot}01$. The values of other required parameters expressed in Appendix A are calculated to be: $l = 111{\cdot}8$m, $\alpha_2 = 0{\cdot}0611391$, $\beta_2 = 0{\cdot}0302985$, $\gamma_2 = 0{\cdot}117431$, $\alpha_3 = 0{\cdot}0605974$, $\eta_3 = 0{\cdot}117431$, $\gamma_3 = 0{\cdot}117431$. For given $\mu_i (i = 2, 3)$, σ_2 and f_3 are, respectively, the damping parameters, the detuning parameters for external excitation and the excitation amplitude. The steady state response of the system is obtained by solving equations (28) numerically using Newton–Raphson's method. The stability and bifurcation of the trivial and non-trivial responses are also studied from the eigenvalues of the Jacobian matrix. As the frequency (or forced) response curves are found to be symmetrical about the σ_2-axis or f_3-axis, only the positive sides of the response curves are shown in Figures 2 and 3. The solid and dashed lines stand for the stable and unstable branches. Here, the effects of damping, amplitude and the frequency of the excitation on the system response are studied.

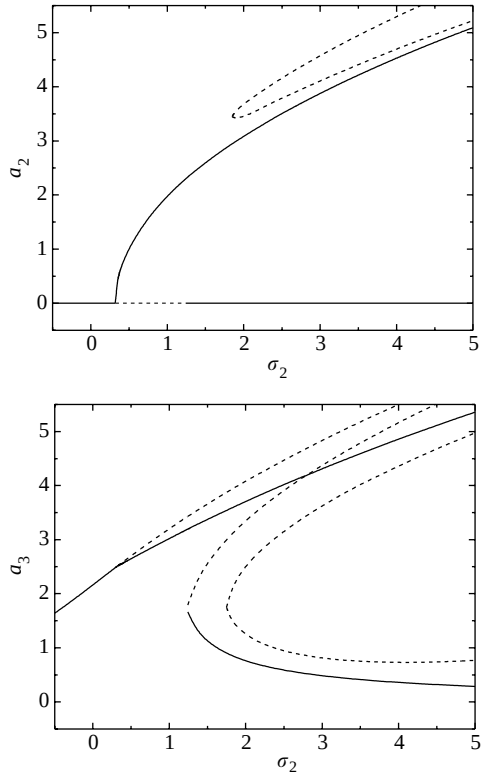

Figure 3. Frequency–response curve for a cable for the case of a primary resonance of the first mode: $f_3 = 0{\cdot}45$, $\mu_2 = 0{\cdot}025$, $\mu_3 = 0{\cdot}1$.

Solutions of equations (28) can be classified into two types, which are $a_2 = 0$, $a_3 \neq 0$ and $a_2 \neq 0$, $a_3 \neq 0$. The steady state frequency–response curve for system with $f_3 = 0{\cdot}85$, $\mu_2 = 0{\cdot}2$ and $\mu_3 = 0{\cdot}2$ is shown in Figure 2. In the trivial branch, pitchfork bifurcation occurs at $\sigma_2 = 0{\cdot}512$, and the trivial solution loses its stability via a pitchfork bifurcation. An additional branch of stable non-trivial solution exists in the frequency–response curve. With an increase in σ_2, a_2 increases rapidly, but a_3 increases slowly. From Figure 2, it can be shown that when $\sigma_2 < 0{\cdot}512$ only the stable trivial solution exists, so the in-planar component of the motion would die out due to the presence of damping. It is also shown from Figure 2 that the responses of equation (27) are similar to the response of the Duffing oscillator with a hardening spring, but there only exists one stable branch for the responses of equation (27). It also shows that the internal resonance has an effect on the stability of the solution. There exist two unstable branches for $\sigma_2 > 2{\cdot}7$, and the saddle node bifurcation at $\sigma_2 = 1{\cdot}81$.

In the case of $f_3 = 0{\cdot}45$, $\mu_2 = 0{\cdot}025$ and $\mu_3 = 0{\cdot}1$, frequency–response curves are plotted as shown in Figure 3, which is similar to Figure 2. However, it is obvious that the pitchfork bifurcation and the saddle node bifurcation points move forward, and the amplitudes of the motion are somehow decreased. The sag will lead to the result that a_2 is always smaller than a_3 for a given σ_2. And a_2 and a_3 will finally be equal to each other without sag [11].

The variations of the response amplitude a_2 and a_3 with the amplitude of the excitation f_3 are shown in Figures 4 and 5, and there exists a critical value of f_3, respectively, in them. From Figures 4 and 5, it can be shown that when f_3 is larger than the critical value, the

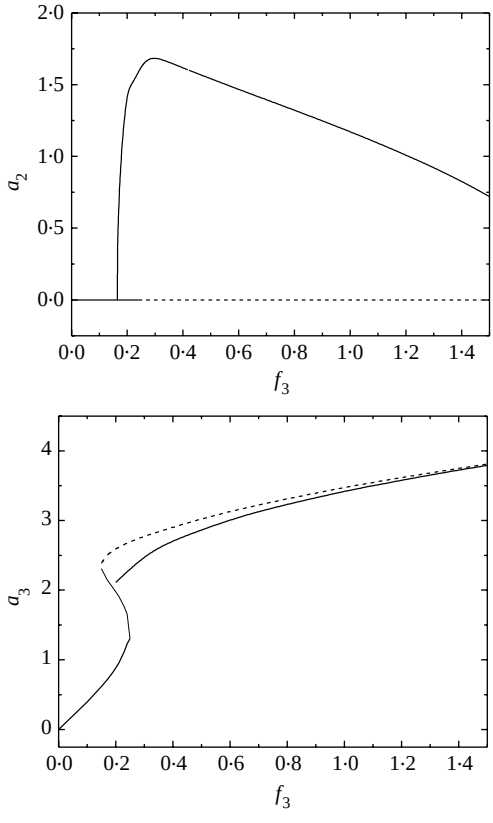

Figure 4. Variation of the amplitude of the first mode with amplitude of the excitation: $\sigma_2 = 0{\cdot}8$, $\mu_2 = 0{\cdot}2$, $\mu_3 = 0{\cdot}2$.

amplitude of the in-planar component begins to grow and the amplitude of the in-planar component grows rapidly as f_3 changes slightly. After the amplitude of the in-planar arrives at the largest value, it decreases gradually and dies out at last as f_3 increases.

Next, the predicted motion is described as the σ_2 is varied slowly up. Referring to Figure 2, starting with a negative value of σ_2, we expect to initiate out-planar motion. Then as σ_2 increases, the amplitudes of the two components of the motion move from P to A and O to F. When $\sigma_2 = 0{\cdot}512$, the amplitude of the in-planar component begins to grow, and as σ_2 increases, the two amplitudes increase. When $\sigma_2 = 7{\cdot}615$ (not included in Figure 2), the motion becomes unstable, and the jump phenomenon can be seen. The motion changes from non-planar back to out-planar. Reversing the procedure, we start with a large value of σ_2. Again, the initiative out-planar motion is expected. As σ_2 decreases, the amplitude of the two components move from C to D and from H to I; when $\sigma_2 = 1{\cdot}81$, the non-planar motion is expected and the jump phenomenon is seen again. As the σ_2 decreases, the amplitude of the in-planar component decreases. When $\sigma_2 = 0{\cdot}512$, the in-planar component is zero, and the motion is out-planar again.

In order to verify the analytic results, the equations of motions were numerically integrated using a fourth order Runge–Kutta algorithm. In the following two cases, the numerical results were in accordance with the theoretical predictions. The numerical responses presented in the following are typical of the computed simulations and correspond to the system with $f_3 = 0{\cdot}85$, $\mu_2 = 0{\cdot}2$ and $\mu_3 = 0{\cdot}2$, whose response curves were

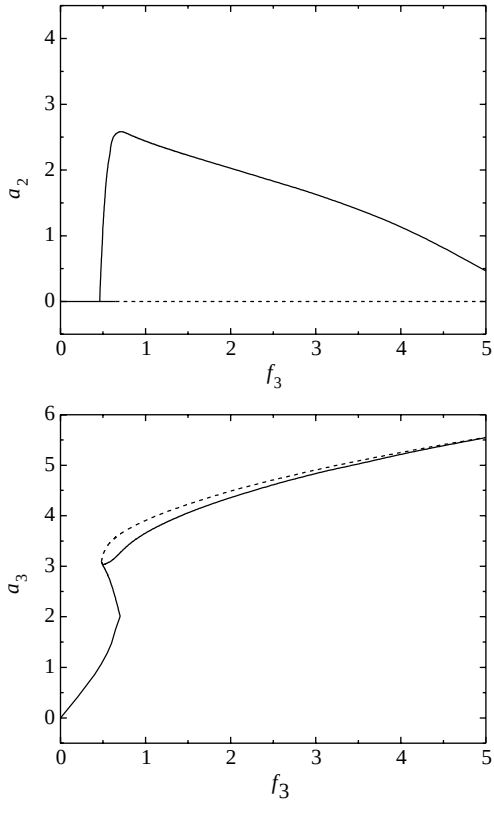

Figure 5. Variation of the amplitude of the first mode with amplitude of the excitation: $\sigma_2 = 1{\cdot}5$, $\mu_2 = 0{\cdot}15$, $\mu_3 = 0{\cdot}5$.

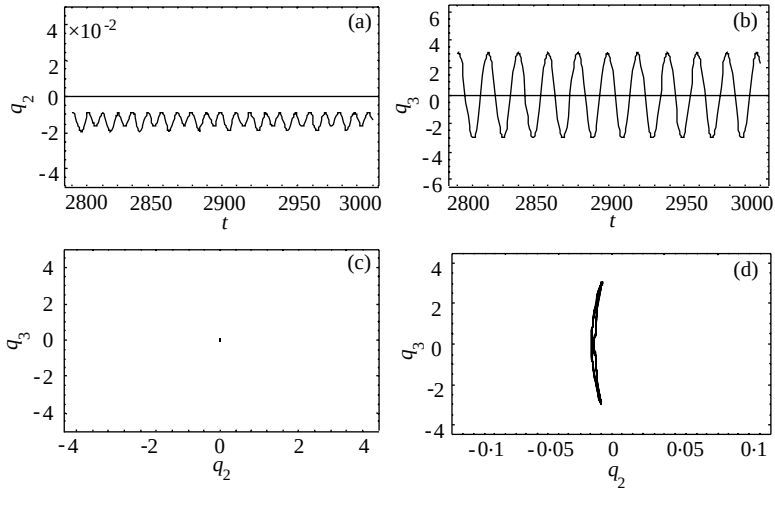

Figure 6. Stable motion $\sigma_2 = 0{\cdot}7$.

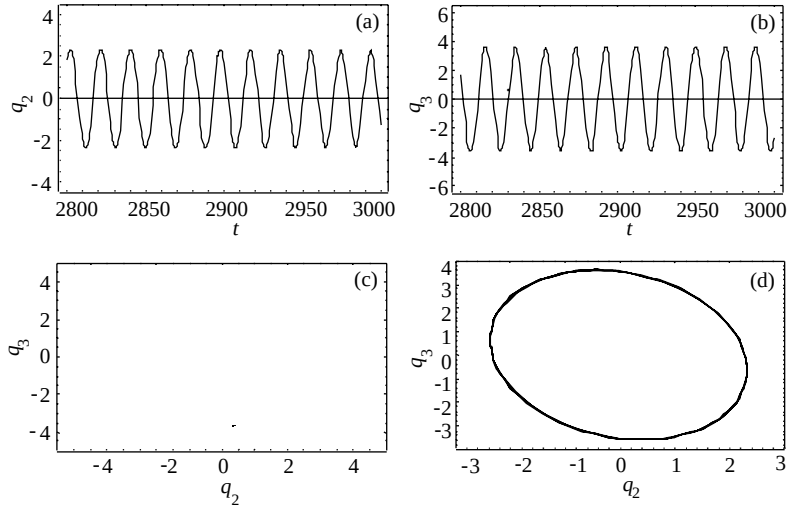

Figure 7. Stable motion $\sigma_2 = 1{\cdot}4$.

presented in Figure 2. Figures 6 and 7 present the response of the cable, one for $\sigma_2 = 0{\cdot}45$, the other for $\sigma_2 = 1{\cdot}4$. A four-dimensional Poincaré map of the response was constructed by sampling the dynamic at multiples of the period of the forcing function, and the projections of Poincaré map in the q_2–q_3 plane are indicated in Figures 6(c) and 7(c). As expected, the periodic motion is represented by one point in the projection of the Poincaré map. Figures 6(a) and 7(a) show the time history of the motion in-planar, which indicate that there only exists the out-planar pendulation for $\sigma_2 < 0{\cdot}512$ and the coupled motion between the out-planar pendulation and the in-planar vibration for $\sigma_2 > 0{\cdot}512$.

4. CONCLUSIONS

The non-linear response of an elastic cable which is simply supported is studied using the method of reduce and multiple scales. Besides, the stability and bifurcation of the trivial and non-trivial branches for different values of damping, amplitude and frequency of excitation are analyzed. Pitchfork bifurcation and saddle node bifurcation are observed. Moreover, the coupled dynamic features between the out-planar pendulation and the in-planar vibration of an elastic cable are analyzed, which are verified by numerical integrations using a fourth order Runge–Kutta algorithm. Meanwhile, the sag's influence on the amplitude of motion is analyzed in this paper.

ACKNOWLEDGMENTS

The work described in this paper was supported by the Natural Science Foundation of Hunan Province Grant No. 99JJY2084. The authors would like to thank the referees for their constructive suggestions.

REFERENCES

1. H. YAMAGUCHI, T. MIGATA and M. ITO 1981 *Proceedings of Japan Society of Civil Engineers* **308**, 424–427. Time response analysis of a cable under harmonic excitation (in Japanese).

2. Z. YU and Y. L. XU 1998 *Journal of Sound Vibration* **214**, 659–673. Mitigation of three-dimensional vibration of inclined sag cable using discrete oil-dampers—I. formulation.
3. P. HAGEDORN and B. SCHAFER 1980 *International Journal of Non-linear Mechanics* **15**, 333–340. On nonlinear free vibrations of an elastic cable.
4. G. V. RAO and R. IYENGAR 1991 *Journal of Sound and Vibration* **149**, 25–41. Internal resonance and non-linear response of a cable under periodic excitation.
5. K. TAKAHASHI 1991 *Journal of Sound and Vibration* **144**, 323–330. Dynamic stability of cables subjected to an axial period load.
6. N. C. PERKINS 1992 *International Journal of Non-linear Mechanics* **27**, 233–250. Modal interactions in the nonlinear response of elastic cable under parametric/external excitation.
7. M. P. BENITO, Y. FUJINO and A. SULEKH 1993 *Journal of Structural Engineering* **119**, 1961–1979. Estimation curve for modal damping in stay cables with viscous damper.
8. F. BENEDETHNI, G. REGA and R. ALAGGIO 1995 *Journal of Sound and Vibration* **182**, 775–798. Non-linear oscillations of a four-degree-of-freedom model of a suspended cable under multiple internal resonance conditions.
9. Y. Y. ZHAO, L. H. WANG, D. L. CHEN and L. Z. JIANG 2001 *Journal of Hunan University* (*Natural Science*) **28**, 90–96. The three-dimensional non-linearity dynamic analysis of inclined-cable (in Chinese).
10. Y. Y. ZHAO 2000 *Ph.D. Thesis*, *Hunan University*, *Changsha*. The Theoretical Model of Non-linear Dynamic for Long-span Cable-stayed Bridge (in Chinese).
11. A. H. NAYFEH and D. T. MOOK 1979 *Nonlinear Oscillations*. New York: Wiley Inter-Science Publication.
12. A. H. NAYFEH 1981 *Introduction to Perturbation Techniques*. New York: Wiley Inter-Science.
13. L. H. WANG 2001 *Dissertation*, *Hunan University*, *Changsha*. The non-linear dynamic analysis of an elastic cable (in Chinese).

APPENDIX A

The coefficients in equations (14) are given as follows:

$$b_1 = \int_0^l \varphi_2^2 \,\mathrm{d}x$$

$$b_2 = -\frac{l}{H_0}\int_0^l \frac{\partial}{\partial x}\left[N_0\left(1-\frac{y_x^2}{2}\right)\varphi_{2x} - (N_0 - EA)y_x\int_0^l y_x\varphi_{2x}\,\mathrm{d}x\right]\varphi_2\,\mathrm{d}x,$$

$$b_3 = \frac{l}{H_0}\int_0^l \frac{\partial}{\partial x}\left[(N_0 - EA)\varphi_{2x}\int_0^l y_x\varphi_{2x}\,\mathrm{d}x + \frac{(N_0 - EA)\mathrm{y}_x}{2}\int_0^l \varphi_{2x}^2\,\mathrm{d}x\right]\varphi_2\,\mathrm{d}x,$$

$$b_4 = \frac{l}{H_0}\int_0^l \frac{\partial}{\partial x}\left[\frac{(N_0 - EA)y_x}{2}\int_0^l \varphi_{3x}^2\,\mathrm{d}x\right]\varphi_2\,\mathrm{d}x,$$

$$b_5 = \frac{l}{H_0}\int_0^l \frac{\partial}{\partial x}\left[\frac{(N_0 - EA)\varphi_{2x}}{2}\int_0^l \varphi_{2x}^2\,\mathrm{d}x\right]\varphi_2\,\mathrm{d}x,$$

$$b_6 = \frac{l}{H_0}\int_0^l \frac{\partial}{\partial x}\left[\frac{(N_0 - EA)\varphi_{2x}}{2}\int_0^l \varphi_{3x}^2\,\mathrm{d}x\right]\varphi_2\,\mathrm{d}x,$$

$$\zeta_2 = \int_0^l c_2\varphi_2^2\,\mathrm{d}x,$$

$$c_1 = \int_0^l \varphi_3^2\,\mathrm{d}x,$$

$$c_2 = -\frac{l}{H_0}\int_0^l \frac{\partial}{\partial x}\left[N_0\left(1-\frac{y_x^2}{2}\right)\varphi_{3x}\right]\varphi_3\,\mathrm{d}x$$

$$c_3 = \frac{l}{H_0}\int_0^l \frac{\partial}{\partial x}\left[(N_0 - EA)\varphi_{3x}\int_0^l y_x\varphi_{2x}\,\mathrm{d}x\right]\varphi_3\,\mathrm{d}x$$

$$c_4 = \frac{l}{H_0}\int_0^l \frac{\partial}{\partial x}\left[\frac{(N_0 - EA)}{2}\varphi_{3x}\int_0^l \varphi_{2x}^2\,\mathrm{d}x\right]\varphi_3\,\mathrm{d}x$$

$$c_5 = \frac{l}{H_0}\int_0^l \frac{\partial}{\partial x}\left[\frac{(N_0 - EA)}{2}\varphi_{3x}\int_0^l \varphi_{3x}^2\,\mathrm{d}x\right]\varphi_3\,\mathrm{d}x,$$

$$\zeta_3 = \int_0^1 c_3\varphi_3^2\,\mathrm{d}x,$$

$$Q(t) = \int_0^l F(x,t)\,\varphi_3\,\mathrm{d}x.$$

APPENDIX B

(1) The derivation of equations (4) from equations (1).

First, we derive equations (3) as follows:

$$\frac{\mathrm{d}x}{\mathrm{d}s} = \frac{1}{\sqrt{(1+u)^2 + (w_x + y_x)^2 + v_x^2}} \tag{B1}$$

and

$$(1+u_x)^2 + (w_x + y_x)^2 + v_x^2 = 1 + 2u_x + u_x^2 + w_x^2 + y_x^2 + w_x y_x + v_x^2 = 1 + t,$$

where

$$t = 2u_x + u_x^2 + w_x^2 + y_x^2 + w_x y_x + v_x^2, \quad t \ll 1 \tag{B2}$$

at the same time using the equation $(1+\varepsilon)^{-1/2} = 1 - \varepsilon/2 + 3\varepsilon^2/8 + O(\varepsilon^2)$ and the Taylor series expansion and retaining the lower order non-linear terms, equation (B1) can be expressed by

$$\begin{aligned}\frac{\mathrm{d}x}{\mathrm{d}s} &= \frac{1}{\sqrt{(1+u_x)^2 + (w_x + y_x)^2 + v_x^2}} = 1 - \frac{t}{2} + \frac{3t^2}{8} + O(\varepsilon^2)\\ &= 1 - u_x - \frac{u_x^2}{2} - \frac{w_x^2}{2} - \frac{y_x^2}{2} - \frac{v_x^2}{2} - w_x y_x + \frac{3(2u_x)^2}{8} + O(\varepsilon^2)\\ &= 1 - u_x - \frac{u_x^2}{2} - \frac{w_x^2}{2} - \frac{y_x^2}{2} - \frac{v_x^2}{2} - w_x y_x + \frac{3u_x^2}{2} + O(\varepsilon^2)\\ &= 1 - e - \frac{y_x^2}{2} + O(\varepsilon^2) \approx 1 - e - \frac{y_x^2}{2}\end{aligned} \tag{B3}$$

which are equations (3). The derivation of equations (4) from equations (1) is listed as below. As an explanation, here the detailed derivation of equation (1a) is given as follows: From equation (1a) we can obtain

$$\frac{\partial}{\partial x}\left\{\left[(N_0 - EA)\frac{\mathrm{d}x}{\mathrm{d}s} + \frac{1}{\sqrt{1 + y_x^2}}EA\right](1 + u_x)\right\} = \rho A u_{tt}. \tag{B4}$$

Substituting equations (B3) into equations (B4) and using the Taylor series expansion and retaining the lower order non-linear terms, we can obtain

$$u_{tt} - \frac{1}{\rho A}\frac{\partial}{\partial x}\left\{\left[(N_0 - EA)\left(1 - e - \frac{y_x^2}{2}\right) + \left(1 - \frac{y_x^2}{2}\right)EA\right](1 + u_x)\right\} \approx 0. \tag{B5}$$

Therefore, we can obtain

$$\begin{aligned} u_{tt} + \frac{1}{\rho A}\frac{\partial}{\partial x}[(N_0 - EA)e] - \frac{1}{\rho A}\frac{\partial}{\partial x}\left[N_0\left(1 - \frac{y_x^2}{2}\right)u_x\right] + \frac{1}{\rho A}\frac{\partial}{\partial x}[(N_0 - EA)u_x e] \\ - \frac{1}{\rho A}\frac{\partial}{\partial x}\left[N_0\left(1 - \frac{y_x^2}{2}\right)\right] = 0, \end{aligned} \tag{B6}$$

where

$$- \frac{1}{\rho A}\frac{\partial}{\partial x}\left[N_0\left(1 - \frac{y_x^2}{2}\right)\right]$$

is independent of time t, thus it can be dealt with by co-ordinates translation. For simplicity in this paper, this term can be neglected. So we can obtain

$$u_{tt} + \frac{1}{\rho A}\frac{\partial}{\partial x}[(N_0 - EA)e] - \frac{1}{\rho A}\frac{\partial}{\partial x}\left[N_0\left(1 - \frac{y_x^2}{2}\right)u_x\right] + \frac{1}{\rho A}\frac{\partial}{\partial x}[(N_0 - EA)u_x e] = 0, \tag{B7}$$

which is equation (4a). Similarly, the derivation of equation (4b) can be obtained from equation (1b), with

$$-\frac{1}{\rho A}\frac{\partial}{\partial x}\left[N_0\left(1 - \frac{y_x^2}{2}\right)y_x\right]$$

being neglected. Also, equation (4c) can be derived from equation (1c) similarly.

(2) Equations (6) and equation (7) are obtained as follows:
Introducing the non-dimensional time t^* defined as

$$t^* = \sqrt{\frac{H_0}{\rho A l}}\, t. \tag{B8}$$

Therefore,

$$\frac{\mathrm{d}}{\mathrm{d}t} = \frac{1}{\sqrt{\rho A l / H_0}}\frac{\mathrm{d}}{\mathrm{d}t^*} \tag{B9}$$

$$\frac{\mathrm{d}^2}{\mathrm{d}t^2} = \frac{1}{\sqrt{\rho A l / H_0}}\frac{\mathrm{d}}{\mathrm{d}t}\left(\frac{\mathrm{d}}{\mathrm{d}t^*}\right) = \frac{1}{\sqrt{\rho A l / H_0}}\frac{\mathrm{d}}{\mathrm{d}t^*}\left(\frac{\mathrm{d}}{\mathrm{d}t^*}\right)\frac{\mathrm{d}t^*}{\mathrm{d}t} = \frac{H_0}{\rho A l}\frac{\mathrm{d}^2}{\mathrm{d}t^{*2}}. \tag{B10}$$

So u_{tt} can be written as

$$u_{tt} = \frac{\partial^2 u}{\partial t^2} = \frac{H_0}{\rho A l}\frac{\partial^2 u}{\partial t^{*2}} = \frac{H_0}{\rho A l}u_{t^*t^*}. \tag{B11}$$

Substituting equation (B11) into equation (B7), we can obtain

$$\frac{H_0}{\rho A l}u_{t^*t^*} + \frac{1}{\rho A}\frac{\partial}{\partial x}[(N_0 - EA)e] - \frac{1}{\rho A}\frac{\partial}{\partial x}\left[N_0\left(1 - \frac{y_x^2}{2}\right)u_x\right] + \frac{1}{\rho A}\frac{\partial}{\partial x}[(N_0 - EA)u_x e] = 0. \tag{B12}$$

So

$$u_{t^*t^*} + \frac{l}{H_0}\frac{\partial}{\partial x}[(N_0 - EA)e] - \frac{l}{H_0}\frac{\partial}{\partial x}\left[N_0\left(1 - \frac{y_x^2}{2}\right)u_x\right] + \frac{l}{H_0}\frac{\partial}{\partial x}[(N_0 - EA)u_x e] = 0. \tag{B13}$$

If the * notation is disposed for the convenience of writing, we can obtain

$$u_{tt} + \frac{l}{H_0}\frac{\partial}{\partial x}[(N_0 - EA)e] - \frac{l}{H_0}\frac{\partial}{\partial x}\left[N_0\left(1 - \frac{y_x^2}{2}\right)u_x\right] + \frac{l}{H_0}\frac{\partial}{\partial x}[(N_0 - EA)u_x e] = 0, \tag{B14}$$

which is equation (6a). Similarly, equations (6b) and (6c) can be obtained.

If we only consider the lower order transverse modes, no interaction will occur between these transverse modes and the longitudinal modes, and the longitudinal inertia u_{tt} can be neglected. As a consequence from equation (B14), we can obtain

$$\frac{l}{H_0}\frac{\partial}{\partial x}[(N_0 - EA)e] - \frac{l}{H_0}\frac{\partial}{\partial x}\left[N_0\left(1 - \frac{y_x^2}{2}\right)u_x\right] + \frac{l}{H_0}\frac{\partial}{\partial x}[(N_0 - EA)u_x e] \approx 0 \tag{B15}$$

so

$$\frac{\partial}{\partial x}[(N_0 - EA)e - N_0\left(1 - \frac{y_x^2}{2}\right)u_x + (N_0 - EA)u_x e] \approx 0 \tag{B16}$$

if defining $P(x, t) = (N_0 - EA)e - N_0(1 - y_x^2/2)u_x + (N_0 - EA)u_x e$, we can obtain

$$\frac{\partial}{\partial x}P(x, t) \approx 0, \tag{B17}$$

therefore, we can view $P(x, t)$ as the function of time t, then

$$(N_0 - EA)e - N_0\left(1 - \frac{y_x^2}{2}\right)u_x + (N_0 - EA)u_x e \approx P(t) \tag{B18}$$

which is the equation (7).